BIOCHEMISTRY
including biophysical chemistry & molecular biology

Article

pubs.acs.org/biochemistry

Stability of the S_3 and S_2 State Intermediates in Photosystem II Directly Probed by EPR Spectroscopy

Guiying Chen,[†] Guangye Han,[†,‡] Erik Göransson, Fikret Mamedov, and Stenbjörn Styring*

Molecular Biomimetics, Department of Photochemistry and Molecular Science, Ångström Laboratory, Box 523, Uppsala University, SE-751 20 Uppsala, Sweden

Supporting Information

ABSTRACT: The stability of the S_3 and S_2 states of the oxygen evolving complex in photosystem II (PSII) was directly probed by EPR spectroscopy in PSII membrane preparations from spinach in the presence of the exogenous electron acceptor P*p*BQ at 1, 10, and 20 °C. The decay of the S_3 state was followed in samples exposed to two flashes by measuring the split S_3 EPR signal induced by near-infrared illumination at 5 K. The decay of the S_2 state was followed in samples exposed to one flash by measuring the S_2 state multiline EPR signal. During the decay of the S_3 state, the S_2 state multiline EPR signal first increased and then decreased in amplitude. This shows that the decay of the S_3 state to the S_1 state occurs via the S_2 state. The decay of the S_3 state was biexponential with a fast kinetic phase with a few seconds decay half-time. This occurred in 10−20% of the PSII centers. The slow kinetic phase ranged from a decay half-time of 700 s (at 1 °C) to ∼100 s (at 20 °C) in the remaining 80−90% of the centers. The decay of the S_2 state was also biphasic and showed quite similar kinetics to the decay of the S_3 state. Our experiments show that the auxiliary electron donor Y_D was oxidized during the entire experiment. Thus, the reduced form of Y_D does not participate to the fast decay of the S_2 and S_3 states we describe here. Instead, we suggest that the decay of the S_3 and S_2 states reflects electron transfer from the acceptor side of PSII to the donor side of PSII starting in the corresponding S state. It is proposed that this exists in equilibrium with Y_Z according to $S_3Y_Z \Leftrightarrow S_2Y_Z^{\bullet}$ in the case of the S_3 state decay and $S_2Y_Z \Leftrightarrow S_1Y_Z^{\bullet}$ in the case of the S_2 state decay. Two kinetic models are discussed, both developed with the assumption that the slow decay of the S_3 and S_2 states occurs in PSII centers where Y_Z is also a fast donor to P_{680}^{+} working in the nanosecond time regime and that the fast decay of the S_3 and S_2 states occurs in centers where Y_Z reduces P_{680}^{+} with slower microsecond kinetics. Our measurements also demonstrate that the split S_3 EPR signal can be used as a direct probe to the S_3 state and that it can provide important information about the redox properties of the S_3 state.

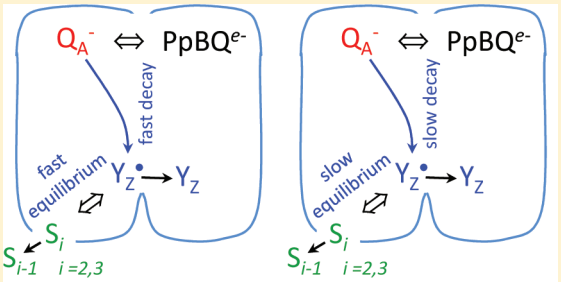

Recombination pathways for the S_3 and S_2 states in Photosystem II

Photosystem II (PSII) in the thylakoid membrane of plants, algae, and cyanobacteria is alone in nature to catalyze light-driven oxidation of water to molecular oxygen.[1,2] Light-driven water oxidation is an energetically demanding and chemically complex reaction. It couples the absorption of single photons to oxidation of two water molecules which is a reaction that involves extraction of four electrons and expulsion of four protons. To manage this, the oxidizing side of PSII (OEC, consisting of redox active tyrosine residue, Y_Z, and Mn_4CaO_5 cluster) carries out unique cyclic redox chemistry, known as the S-state cycle.[3−8]

During catalysis, the OEC cycles through 5 intermediates denoted S_0 to S_4. S_0 is the most reduced state while the S_1 state dominates in the dark. The metastable S_2 and S_3 states both reach oxidizing potentials around +900 mV.[5,8,9] S_4 is a transient state formed during the final step where oxygen is released, and the system returns to the most reduced state, S_0.[6−8]

X-ray crystallography has provided a series[10−12] of sequentially better and better resolved models of PSII, and recently the structure of PSII to 1.9 Å resolution was presented.[12] The structure shows how the many components in the OEC are held together, determines the distance between Y_Z and its hydrogen-bonding partners His_Z and water, clarifies distances and angles between the Ca, Mn, oxygen atoms, and other components, etc. However, the multistep function of the OEC is not solved by structural information alone. Instead, the most detailed experimental information comes from spectroscopic techniques like EPR, X-ray spectroscopy, FTIR, etc.[13−21] However, the present knowledge is lowest for the two S states directly involved in the formation of oxygen, S_3 and S_4. For S_4 there is hardly any clear-cut information at all, reflecting its transient nature.

For the S_3 state the situation is different. This state can be studied by a variety of spectroscopic techniques. However, the data are not conclusive, and the X-ray spectroscopic information is interpretable in two distinct ways, indicating either Mn-centered oxidation[18,19,22] or ligand-centered oxidation[20,21] in the S_2 to S_3 transition. Solution of this difference is important to take further steps to understand this critical

Received: April 24, 2011
Revised: November 23, 2011
Published: November 23, 2011

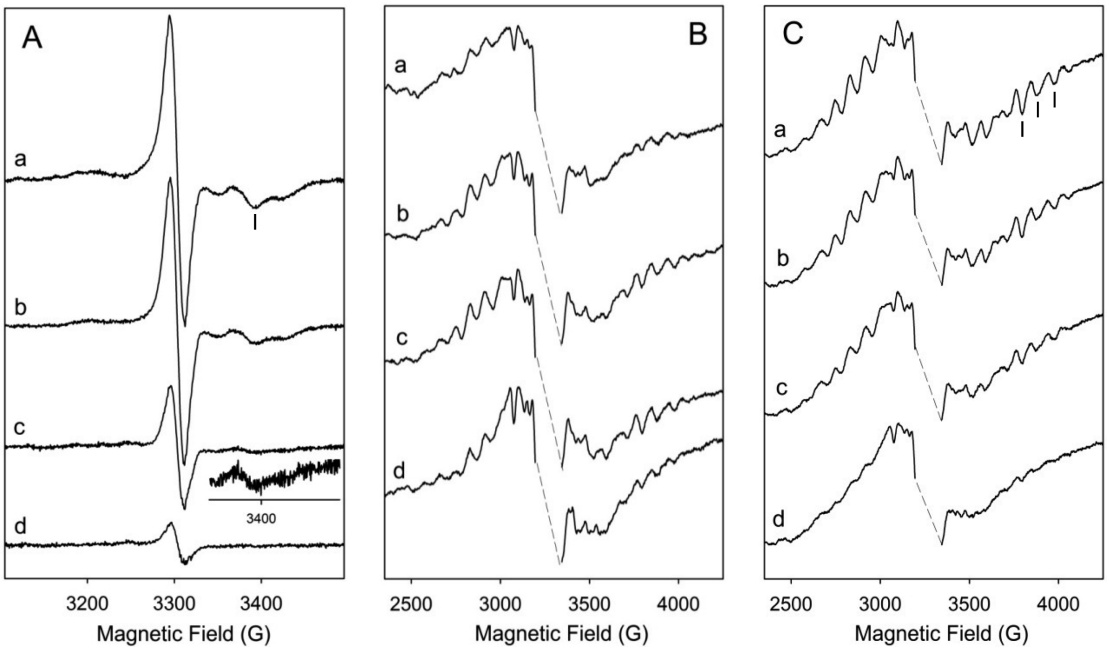

Figure 1. Spectra showing the split S_3 signals (A) and S_2 multiline signals (B, C) recorded in a series of samples during the decay of the S_3 and S_2 state at 20 °C. Synchronized PSII samples were given two flashes (A and B) or one flash (C) and were then incubated in the dark at 20 °C for 0 min (no decay, spectra a), 1 min (spectra b), 5 min (spectra c), and 15 min (spectra d) before freezing (see Materials and Methods for details of this experiment). (A) Split S_3 EPR signals induced by illumination by NIR light for 10 min at 5 K in the presence of 0.5 mM P*p*BQ. The spectra presented are light minus dark difference EPR spectra. The inset under spectrum c shows the high field region of the split S_3 signal amplified 4 times. EPR conditions: microwave power 25 mW, microwave frequency 9.27 GHz, modulation amplitude 10 G, *T* 5 K. (B) S_2 state multiline EPR signals recorded in the same samples as in (A) before the NIR illumination was applied. The large intensity from $Y_D^\bullet$ in the center has been removed for clarity (dashed line). EPR conditions: microwave power 10 mW, microwave frequency 9.27 GHz, modulation amplitude 20 G, *T* 10 K. (C) S_2 state multiline EPR signals recorded in the sample exposed to one flash. EPR conditions are the same as in (B). The vertical bars indicate the field position for the amplitude measurements used in the decay experiments.

intermediate. Direct EPR studies of the S_3 state are very difficult, since the described EPR signals are small, difficult to investigate, and not well understood.[14,16,23−26] Therefore, application of strong spectroscopy to functional investigations of important factors like stability, decay pathways, formation kinetics, pH dependence, etc., has been held back. Instead, much current knowledge is derived from indirect, but ingenious, measurements of flash-induced oxygen evolution yield after application of double-flash techniques or well-designed delay times.[6,27,28]

However, at certain conditions it is possible to detect an EPR signal from the S_3 state. This so-called split S_3 signal (Figure 1A, spectrum a) arises from the magnetic interaction between the $Y_Z^\bullet$ radical and Mn_4CaO_5 cluster.[23,25] It is formed in PSII poised in the S_3 state (after two flashes, for example) after illumination at ultralow temperatures (5 K) which prevents many electron and proton transfer reactions. Illumination at this very low temperature results in the formation of the split S_3 EPR signal which has been assigned to a redox state called $S_2Y_Z^\bullet$.[14,16,23,25,26] The formation of this state does not alter the original distribution of the S states in the sample obtained for example after two flashes and/or after their decay in the dark at room temperature. Simply rising the temperature from 5 to 100 K results in the return of the $S_2Y_Z^\bullet$ state (and consequently the split S_3 signal) to the original S_3 state. Illumination can be made by either visible light or light in the near-infrared region, both creating the same state.[26] When illumination is made by NIR light, the split S_3 signal is very stable, facilitating studies of the signal. We have shown that it can be used in a quantitative manner[29] and have used this property to quantify the miss parameter in the S_2 to S_3 and S_3 to S_0 transitions.[30] The pH dependence of the signal was also recently described and found to be very informative on the situation around Y_Z in the S_3 state.[31]

Thus, the split S_3 signal provides an ideal, but not much used, direct spectroscopic way to study catalytic properties of the S_3 state. In this publication, this EPR signal is applied to analyze the stability of the S_3 state at different temperatures by a direct EPR measurement. This provides a new probe to S_3 which offers the possibility to follow the fate of this critical redox intermediate during various treatments. In addition, the well-known S_2 state multiline signal (Figure 1C, spectrum a) was used to quantify the S_2 state in our samples.[32]

MATERIALS AND METHODS

Preparation of PSII Membranes. PSII membranes (BBY particles) were prepared from green house grown spinach according to refs 33 and 34. Our preparation protocol has been optimized to give a PSII membrane preparation with optimal oscillation characteristics in the EPR measurements. The Chl *a*/*b* ratio was 2.1−2.2, and the activity was 430 ± 10 μmol of oxygen evolution/(mg of Chl h) in a buffer with 25 mM Mes-NaOH (pH 6.3), 400 mM sucrose, 5 mM $MgCl_2$, and 10 mM NaCl at 20 °C under saturating light and in the presence of 0.5 mM PpBQ as electron acceptor. This activity was independent of the presence of 5 mM $CaCl_2$.

EPR Sample Preparation and Synchronization of PSII to the S_1 State. PSII-enriched membranes were diluted to ca. 2 mg Chl/mL and filled into calibrated EPR tubes. Before the flash treatment, full oxidation of Y_D was achieved by exposing

dx.doi.org/10.1021/bi200627j | *Biochemistry* 2012, 51, 138−148

the sample to room light for 5 min. The samples were thereafter dark incubated for 15 min at room temperature before application of a preflash protocol.

The OEC in the samples with fully oxidized Y_D was synchronized to contain an absolute majority of the OEC in the S_1 state by the application of a preflash protocol described in refs 29, 35, and 36 followed by a subsequent dark incubation for 30 min. PpBQ to a final concentration of 0.5 mM (from a stock solution in DMSO, final solvent concentration 3% v/v) was added in darkness at room temperature. Single turnover laser flashes were provided from a Nd:YAG laser from Spectra-Physics, Newport, USA (532 nm, 850 mJ, 6 ns, 1.25 Hz).

Induction of the S_3 and S_2 State and Subsequent Incubation of the EPR Samples. Thirty seconds after the addition of PpBQ, the synchronized PSII samples were transferred to an ethanol bath at a series of temperatures (1, 10, and 20 °C) for 3 min to equilibrate. After temperature equilibration, the samples were immediately exposed to the two saturating single turnover flashes, resulting in samples enriched to ca. 77%, 79%, and 76% in the S_3 state at respective temperatures. The fraction of S_3 centers was determined as in ref 29. The flashed samples were then incubated in the dark at the defined temperature for various periods of time before freezing within 1−2 s in an ethanol−dry ice bath at 200 K. The samples were flushed with argon gas and then transferred to liquid nitrogen. The split S_3 signal was induced in each sample by illumination, directly in the EPR cavity, by NIR light (see below). From the amplitude of the split S_3 signal the decay curve of the S_3 state could be obtained, each sample providing one single time point. Prior to induction of the split S_3 EPR signal, the S_2 state multiline signal was recorded to gain control of the concentration of the S_2 state in each sample. In a parallel set of samples, the decay of the S_2 multiline signal was followed in samples given one flash only (100%, 97%, and 90% of the S_2 state at 1, 10, and 20 °C, respectively[30]).

EPR Spectroscopy and Low-Temperature Illumination Protocol. EPR measurements were performed with a Bruker ELEXYS E500 spectrometer with a SuperX EPR049 microwave bridge and a Bruker SHQ4122 cavity. The spectrometer was equipped with a liquid helium cryostat and temperature controller (ITC502) from Oxford Instruments Ltd. Illumination at 5 K during the EPR measurement was carried out directly into the EPR cavity as in refs 26, 29, and 37. The split S_3 EPR signal was induced by NIR illumination at 830 nm for 10 min at 5 K using a LQC830-135E laser diode, Newport, USA, with a beam-spreader lens placed in front of the EPR cavity window. The NIR light intensity at the cavity window was 67 W/m^2. The light-induced split signals were recorded in darkness immediately after the illumination was terminated to avoid any light-induced heating of the sample. It is important to point out that the split S_3 EPR signal, when induced with NIR light, does not decay at all during the time of the EPR measurement at 5 K.[29,37]

EPR settings are given in the corresponding figure legends. Signal processing and analysis were carried out with the Bruker Xepr 2.4 software. EPR signals were corrected for variations in the sample volume and Chl concentration using the amplitude of the nonsaturated EPR signal from $Y_D^\bullet$ as described in refs 35 and 38. The S_2 state multiline signal and the split S_3 EPR signal induced by NIR light were used to quantify the fraction of PSII in the S_2 and S_3 states, respectively. This was done from the amplitude of respective EPR signal using methods described in ref 29.

It is important for our analysis that the preflash protocol enables us to exclude the S_0 state from all samples in this study. Therefore, the S_1 state alone will make up the remaining centers after the fractions of centers in the S_2 and S_3 states have been determined by the EPR measurements.

RESULTS AND DISCUSSION

Decay of the S_3 and S_2 States. We followed the decay of the S_3 state obtained by providing two flashes to PSII samples synchronized in the S_1 state, at three different temperatures. Figure 1A shows the split S_3 signals recorded in a series of samples taken during the decay of the S_3 state at 20 °C. Immediately after freezing the sample, 76% of PSII was in the S_3 state, resulting in a large split S_3 EPR signal (Figure 1A, spectrum a). The signal decreased in size during incubation of the two flash samples for various times (Figure 1A, spectra b−d).

We also measured the S_2 state multiline signal in the same samples (Figure 1B). This was done prior to the illumination with NIR light. In the sample frozen immediately after the flashes the S_2 state involved 23% of PSII as judged from comparison with the amplitude of the S_2 multiline signal in a sample given one flash at 1 °C where the S_2 state comprises 100% of PSII.[29] The time dependence of the S_2 state multiline signal varied strongly with the temperature for the decay study. During decay of the S_3 state at 20 °C (Figure 1A) the S_2 multiline signal first increased in size and thereafter decreased. This behavior has been observed before[39,40] and reflects a series of reactions. At all times the S_3 state decays back to the S_2 state. This results in decrease of the split S_3 signal and simultaneous formation of the S_2 multiline signal. However, at the same time, PSII centers which were already in the S_2 state decay back to the S_1 state. This results in loss of the S_2 multiline signal. The overall effect can however be that the S_2 multiline signal first increases and thereafter decreases, reflecting both the large fraction of PSII in the S_3 state from the beginning of the experiment and the relative decay time constants of the two S states at the temperature studied (see below).

In the early experiments it was only possible to follow the sequential decay of the S_3 state to the S_2 state and then to the S_1 state by following the S_2 multiline signal (as probe to the S_2 state) and extra inducible S_2 multiline signal (as probe to the S_1 state).[29] The S_3 state was never directly detected but was instead assumed to represent the "rest" of PSII, i.e., those centers that were not detectable in any way by measurement of the S_2 multiline signal.[39,40] Our present approach of using the split S_3 signal as a direct probe to the decay of the S_3 state is a clear advantage and improvement of the spectroscopic methods used to date.

Figure 2A shows the decay data for the S_3 state at three different temperatures (it is important to point out that the data are obtained in the presence of the electron acceptor PpBQ). The S_3 state is stable for a long time at all temperatures, and the decay is faster at higher temperature. The decay parameters for the S_3 state obtained from a two-exponential fit are listed in Table 1. The S_3 state decay was found to be biphasic at the temperatures studied (1, 10, and 20 °C). The smaller fast phase involved 10−20% of the centers that were present in the S_3 state from the start, and the decay half-times were almost similar (10−18 s) at all three temperatures. The dominating slow decay phase involved the remaining PSII centers (80−90% of the centers in the S_3 state) and was dependent on temperature. The decay half-times of the slow phase ranged

dx.doi.org/10.1021/bi200627j | Biochemistry 2012, 51, 138−148

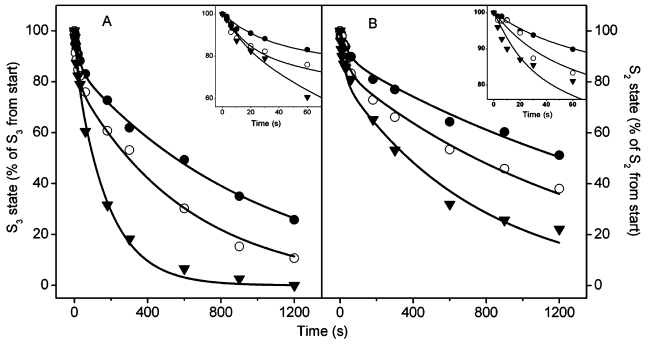

Figure 2. Time course of the decay of the S_3 state (A) and S_2 state (B) in the presence of 0.5 mM PpBQ measured by the intensity of the split S_3 EPR signal (induced by NIR illumination at 5 K) or the S_2 state multiline EPR signal, respectively. The amplitudes of the split S_3 signal and the S_2 state multiline EPR signal measured in a sample frozen immediately after the flashes are set to 100%. The fraction of PSII that actually was in the S_3 (or S_2) state is given in the text. Synchronized PSII samples were given one (S_2 state dominated) or two (S_3 state dominated) flashes and were then incubated in the dark at 1 (●), 10 (○), and 20 (▼) °C for the indicated periods of time before freezing. The inset shows the first 60 s of the decay. The lines represent two exponential fits with parameters shown in Table 1.

from 705 s at 1 °C to 424 s at 10 °C and 124 s at 20 °C. This is quite similar to the slow decay half-time of 210−240 s for the S_3 state found by monitoring only the S_2 state multiline signal in PSII membrane fragments in the presence of PpBQ at room temperature.[39,a] In this early experiment the fast phase was not reported, but it could easily have escaped detection since there are hardly any time points presented from the early part of the decay (compare Figure 2 in ref 39).The data in Figures 1B and 3 (open circles) also show the formation and decay of the S_2 multiline in the same samples that had been given the two flashes. At 1 °C, the concentration of the S_2 state increased during the entire time interval (up to 1200 s), clearly indicating that the formation of the S_2 state was faster than its decay. At 10 °C the S_2 state increased up to 800 s. After this, a small decrease in the amplitude was observed. At 20 °C the situation was different. At early times (to ca. 200 s) the S_2 multiline signal increased rapidly in amplitude. At longer times, however, when the S_3 state was depleted, the decay of the S_2 state was clearly observable during the time course of the measurement (Figure 3C).

The time-dependent decay processes in samples exposed to two flashes (Figure 3) were analyzed assuming that the S_3 state first decayed to the S_2 state, which in its turn decayed to the S_1 state:

$$[S_3] \xrightarrow{k_{S3}} [S_2] \xrightarrow{k_{S2}} [S_1] \quad (1)$$

In this equation, both k_{S3} and k_{S2} involve two decay time constants: one for the fast decay and the other for the slow decay of respectively the S_3 and S_2 states. The decay time constants for the S_3 state could be determined directly from the disappearance of the split S_3 signal (Figure 2A, Table 1). The situation is much more complex for the S_2 state. It is evident that the concentration of the S_2 state, $[S_2]$, at any given time reflects the combined result of two separate processes: the formation of the S_2 state as a result of the S_3 state decay and the subsequent decay of the S_2 state itself. Moreover, the intermediate concentration of the S_2 state in the samples exposed to two flashes involves two S_2 state populations: (i) centers in the S_2 state which never advanced to the S_3 state due to misses after the second flash (ca. 20% in our samples) and (ii) centers in the S_2 state which originate from the decaying S_3 state centers. It is not clear if the stability of these two populations of S_2 state centers is similar or different, and this is a complication in the detailed analysis of these data.

Thus, the intermediate concentration of the S_2 state ($[S_2]$ as measured by the S_2 multiline signal) is determined by the competition between the formation of the S_2 state centers from the decayed S_3 state centers (k_{S3}) and the decay of the S_2 state centers themselves (k_{S2}) irrespective of their origin in (i) or (ii) as discussed above. Taking into account that k_{S2} in each situation can also represent more than single exponential kinetics, analysis of the intermediate state in the sequential reaction is not straightforward. Determination of k_{S3} is clear from direct inspection of the S_3 state decay (Table 1). However, determination of the decay kinetics (k_{S2}) for the S_2 state after two flashes involves too many variables.

Instead of determination of k_{S2} from the S_2 state data alone, it is possible to obtain accurate, apparent S_2 state decay parameters from the S_1 state formation kinetics. The total concentration of the S_2 and S_3 states directly after two flashes represents 100% of the PSII centers in our samples, i.e., $[S_3]_0 + [S_2]_0 = 100\%$ in eq 2. (It is important to note that there were no centers in the S_0 state due to so-called double hits since these are completely abolished in our experiments using nanosecond single turnover laser flashes.) The S_1 state directly after the flashes is negligible within the range of ±3%.[b] However, similar to the decay of the S_3 state, the formation of the S_1 state is a simple process only reflecting the decay of the S_2 state irrespective of the origin for the S_2 state in (i) or (ii). The decay of the S_2 state can thus be determined from the kinetics of the S_1 state formation.

The experimental S_3 and S_2 data in Figure 3 allow us to determine the concentration of the S_1 state at any time $[S_1]_t$,

Table 1. Normalized Amplitudes (a_f, a_s) and Half-Times ($t^f_{1/2}$, $t^s_{1/2}$) of the Fast (f) and Slow (s) Decay Phases of the S_3 (in Samples Given Two Flashes) and S_2 (in Samples Given One Flash) States at Different Temperatures, Measured as the Split S_3 EPR Signal and S_2 Multiline Signal (Figure 2)[a]

	S_3 state decay				S_2 state decay			
temp (°C)	a_f (%)	$t^f_{1/2}$ (s)	a_s (%)	$t^s_{1/2}$ (s)	a_f (%)	$t^f_{1/2}$ (s)	a_s (%)	$t^s_{1/2}$ (s)
1	14	18 ± 4	86	705 ± 19	10/**11**	31 ± 12/**29 ± 7**	90/**89**	1438 ± 59/>**1500**
10	19	12 ± 4	81	424 ± 19	15/**9**	25 ± 8/**13 ± 6**	85/**91**	968 ± 46/**1247 ± 73**
20	11	10 ± 6	89	124 ± 6	18/**10**	16 ± 8/**10 ± 9**	82/**90**	525 ± 36/**543 ± 33**

[a] 100% of the PSII centers were found in the S_2 state after application of one flash, and ca. 76−79% of the PSII centers were found in the S_3 state after two flashes. The data in bold text represent the decay half-times of the S_2 state in the samples exposed to two flashes obtained from exponential fitting of the data in Figure 3 (black squares) as described in the text. In this case the overall amplitude of this decay was set as 100%.

dx.doi.org/10.1021/bi200627j | *Biochemistry* 2012, 51, 138−148

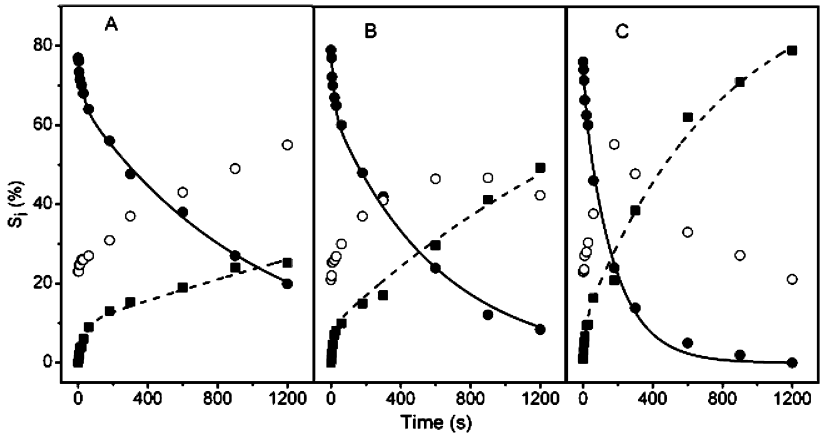

Figure 3. Changes in the amplitudes of the split S_3 (●) and the S_2 state multiline (○) EPR signals during the incubation in the dark of the samples that were exposed to two flashes at 1 (A), 10 (B), and 20 °C (C). The signals were induced and analyzed as described in the Materials and Methods section and in ref 29. The fraction of centers in the S_1 state (■) was estimated with the assumption that they represented the remaining PSII centers after PSII centers being in the S_2 and S_3 states had been accounted for by the EPR measurements according to $[S_1] = 100\% - ([S_3] + [S_2])$. The lines represent two exponential fits of the S_3 state decay (solid line) and the S_1 state rise (dashed line).

and the concentration of the S_1 state (in % of total PSII) can be calculated according to

$$[S_1]_t = ([S_3]_0 + [S_2]_0) - ([S_3]_t + [S_2]_t) \quad (2)$$

The rise of the S_1 state (according to eq 2) is shown in Figure 3. The formation of the S_1 state varied with the temperature: at 1 °C only about 25% of PSII centers decayed to the S_1 state during the entire time course of the experiment (1200 s). At 10 and 20 °C this number was ca. 50% and 80%, respectively (Figure 3). In addition, from eq 1 it is clear that the formation rate of the S_1 state is equal to the overall decay rate of the S_2 state. Thus, combining eqs 1 and 2, the overall decay rate constants of the S_2 state can be determined from the formation rate constants of the S_1 state:

$$-\frac{d[S_2]}{dt} = \frac{d[S_1]}{dt} = k_{S2}[S_1] \quad (3)$$

The results of this analysis are shown in Figure 3 and Table 1. Similarly to the S_3 state decay, two decay phases for the S_2 state in samples exposed to two flashes were observed. At 1 °C, the fast decay phase (half-time about 29 s) involved ~10% of the S_2 centers. At 10 and 20 °C, the fast decay involved similar amounts of the PSII centers with decay half-times of 13 and 10 s, respectively (Table 1). During our 1200 s time window only a small fraction of the slow decaying centers could decay at 1 and 10 °C while the decay was almost complete at 20 °C. The slow phase was evidently temperature dependent, and the half-time was found to range from >1500 s at 1 °C to 1247 s at 10 °C and 543 s at 20 °C (Table 1).

Our data in the samples exposed to two flashes indicate that the S_3 state decays faster than the S_2 state at all three temperatures in samples exposed to two flashes. This can be an inherent property of respective S state, being valid after any number of flashes given to the sample. However, it could also be a flash number dependent effect and for example reflect a different availability for back-reacting electrons from the acceptor side in case of the center being in the S_3 state or the S_2 state. In this case, the first electron would reduce the S_3 state while a second electron is needed to reduce the S_2 state in the same center. One possibility is our use of the electron acceptor PpBQ. This is known to induce a different situation on the acceptor side of PSII after one or two flashes. After one flash, a phenomenon involving the PpBQ semiquinone radical results in oxidation of the nonheme Fe on the acceptor side in a large fraction of PSII.[41] In the subsequent flash, this Fe^{3+} ion actually functions as a very efficient electron acceptor of the electron which is quickly transferred from Q_A^-. Thus, it seems that the acceptor side in PSII should have different reducing abilities after one or two flashes in the presence of PpBQ. This could be reflected in different stability of the S_2 state (while this can hardly be tested for the S_3 state).

We therefore tested whether the decay of the S_2 state was the same in samples given only one flash. In this case only the S_2 state is formed and the decay never involved centers that had been in the S_3 state. The results are shown in Figure 1C, Figure 2B, and Table 1. During the dark incubation the S_2 state decays to the S_1 state, which is reflected by the disappearance of the S_2 multiline signal (Figure 1C). In this experiment the analysis is straightforward. The decay of the S_2 state could also in this situation be fitted by two decay phases: one minor fast phase occurring in tens of seconds and one dominating slow phase (Table 1). The fast phase encompassed 10–18% of the PSII centers that were in the S_2 state from the beginning, and the decay half-times vary from 31 s (1 °C) to 16 s (20 °C) and were thus slightly dependent on temperature. The slow phase involved the remaining 80–90% of PSII centers. This phase was temperature dependent and extremely slow at 1 °C (half-time of 1438 s). At 10 and 20 °C the decay was faster and followed decay half-times of 968 and 525 s, respectively (Table 1).

Thus, we can conclude that the kinetic behavior of the S_2 state formed in PSII sample after one or two flashes is strikingly similar. The S_2 state decays in both cases with two phases. Approximately 10% of the PSII centers decay in a fast process. The rest of the S_2 centers decays in the many minutes time scale. There seems to be little, if any, effect on the S_2 state decay from differences induced by the use of the PpBQ electron acceptor in combination with one or two flashes. In addition, the S_2 state decays slower than the S_3 state, irrespective of temperature or the number of flashes given to the sample.

Analysis of the Biphasic Decay Behavior of the S_3 and S_2 States. Literature data on the stability of the S_2 and S_3

dx.doi.org/10.1021/bi200627j | *Biochemistry* 2012, 51, 138–148

Scheme 1. Two Models That Show Formation and Recombination Pathways for the S_3 State (Similar Models Can Be Employed for the S_2 State) Involving Equilibrium Reactions with Y_Z and P_{680}[a]

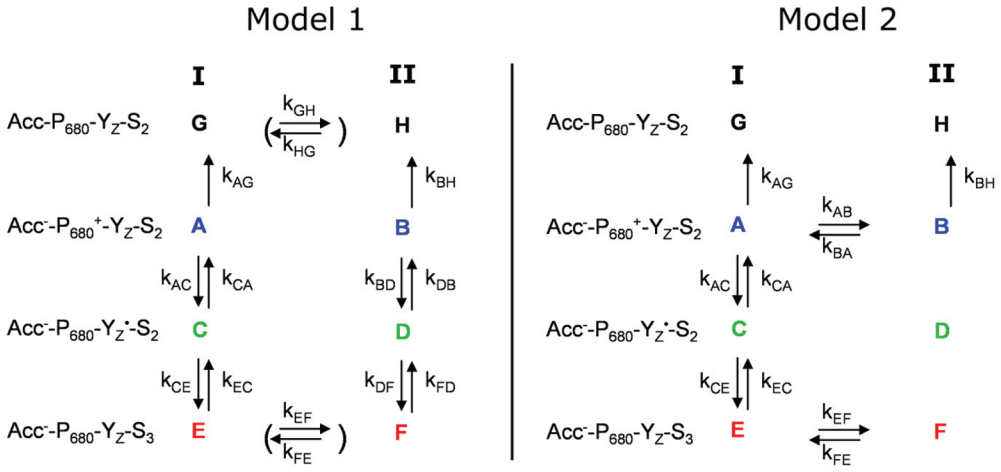

[a]In model 1, the biexponential behavior in the S_2 and S_3 state decays is explained by the existence of two fractions of PS II that do not interchange over the time scale of the experiment. Populations I and II could be in equilibrium on longer time scales (i.e., several minutes). If existing, this equilibrium should exist both between intermediates G and H (top reaction, before the flash) or intermediates E and F (bottom reaction, before the flash). In model 2, the biexponential behavior in reduction of P_{680}^+ ($P_{680}^+-Y_Z \rightarrow P_{680}-Y_Z^\bullet$) comes from that there is two populations (I and II) of $P_{680}^+-Y_Z$ that interchange. Population I reacts fast in intermediate A ($t_{1/2}$ = 200 ns), while population II has to go via intermediate A to form $P_{680}-Y_Z^\bullet$. The difference between the intermediates A and B could be the H-bonding pattern around Y_Z as indicated in Scheme 2. The biexponential behavior for the decay of S_3 back to S_2 is explained by a slow equilibrium between two different states that both show the split S_3 EPR signal (E and F). Numerical solutions to both models are presented in the Supporting Information. However, there are many unknown parameters in both kinetic schemes, indicating that there might exist several different numerical solutions in the kinetic modeling.

states go back to the original experiments which established the concept of the S cycle in water oxidation.[6] These measurements of the flash-induced oxygen yield were performed in intact alga[42,43] or chloroplast/thylakoid membrane preparations[44,45] and reported decay times in the few minutes time scale. Later, the multiline EPR signal from the S_2 state as a direct spectroscopic probe to the S_2 state (and an indirect probe to both the S_1 and S_3 states) was shown to be useful in determination of the decay kinetics of the S_2 and S_3 states.[39]

These earlier measurements did not allow full kinetic resolution of the decay kinetics in either S state. Messinger et al.[46] reported two decay phases in isolated thylakoid membranes from spinach. In this type of preparation no detergent treatment is required, and the acceptor side of PSII (specifically the Q_B site) is usually considered to be more intact if compared to the PSII membrane preparations.[46] In this experiment, which was performed at pH 7.0, the S_3 state was measured indirectly by measuring the oxygen yield induced by a flash train while delaying the time between the first two and consecutive flashes. At 20 °C the S_3 state decayed with two phases, with half-times of 7 s (28%) and 94 s (72%). It was also reported that the S_2 state decayed with half-times of 11 s (35%) and 75 s (65%), and it was shown that both the S_3 and S_2 states were more stable at lower temperatures.[46] These results are similar to our results with respect to the resolution of two decay phases. However, the experiments are not entirely comparable. Our experiments were performed in PSII membrane preparations which were obtained after the mild treatment with Triton X100.[34] Such treatment together with use of sufficient amount of electron acceptor (0.5 mM PpBQ) should minimize any impairment (if at all present) of the Q_B site in our preparation. The different pH's used (pH 6.3 here and pH 7.0 in ref 46) and our introduction of PpBQ as external acceptor are critical differences since the decay of the S_3 and S_2 states is likely to involve pH-dependent components originating from the OEC and Y_Z, in addition to the involvement of electrons from the acceptor side of PSII. Moreover, in ref 46 it was not possible to distinguish between the fast decay kinetics and the reaction where reduced Y_D was involved.

The origin of the two decay phases is not completely understood. They can have different origin dependent on S state and the redox status of the sample. It is normally assumed that the slow phase represents the kinetics of the S_3 state (or the S_2 state) decay by recombination with the acceptor side via redox equilibriums involving P_{680}^+;[47,48] see below for a detailed discussion. Also, reduction of the higher S states by other PSII components or exogenous reductants has been discussed.[28,46,49]

The fast phase has been proposed to reflect the reduction of the S_3 state (or the S_2 state) by Y_D.[28,46] This idea originates from investigations of the interesting situation when Y_D is present in its reduced form. In this case, both the S_2 and S_3 state are reduced from Y_D in biphasic, pH, and temperature dependent reactions that occur in the few seconds time range,[9,28,40,45,50] i.e., much faster than the fast phase we have described here. These reactions have been observed in thylakoids for example after very long dark incubation[9,28,47,51] but have been best studied in PSII membranes by EPR where the oxidation of Y_D can readily be followed by kinetic EPR spectroscopy.[9,40,50]

However, we can exclude involvement of reduced Y_D in our study. The reason is that full oxidation of Y_D is ensured by our preflash protocol. The amplitude of $Y_D^\bullet$ was controlled by EPR in all samples, at all stages in every single experiment. We have no indications that any reduced Y_D was ever present during the decay experiments we describe here. Thus, Y_D was fully oxidized from the start of the experiment. Reduced Y_D can therefore be excluded as decay partner for any of S_2 or S_3, also

dx.doi.org/10.1021/bi200627j | Biochemistry 2012, 51, 138−148

Scheme 2. Proposed Hydrogen Bond Pattern for Y_Z[a]

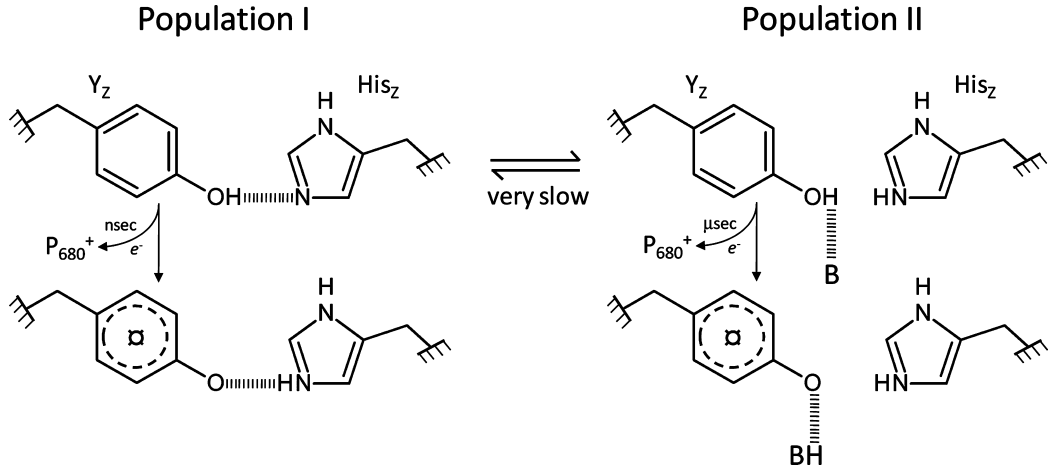

[a]In population I in Scheme 1 electron transfer from Y_Z to P_{680}^+ occurs in the nanosecond time regime. This is thought to reflect that the phenolic proton exists in a well-tuned hydrogen bond to His_Z which allows proton displacement and Y_Z oxidation even at 5 K. In our models 1 and 2 (Scheme 1) we propose that decay of the S_3 state is slow ($t_{1/2} \approx 120$ s at 20 °C) in PSII centers with this mode of hydrogen bond around Y_Z. In population II in Scheme 1, electron transfer from Y_Z to P_{680}^+ occurs in the microsecond time regime. This is thought to reflect that the phenolic proton is less well connected to a neighboring base[52] that is not His_Z. This situation prevents proton displacement and Y_Z oxidation at 5 K. In our models 1 and 2 (Scheme 1) we propose that decay of the S_3 state is fast ($t_{1/2} \approx 10$ s at 20 °C) in PSII centers with this mode of hydrogen bond around Y_Z.

for the fast decay phase with $t_{1/2} \approx 10-15$ s that involved 10–20% of PSII (Table 1).

In our experiments with two flashes, we were also able to observe not only decay of the S_3 state (observed as the split S_3 signal, Figure 1A) but also the appearance and sequential decay of the S_2 state (observed as the S_2 multiline signal, Figure 1B). Both occurred with biphasic kinetics which would have been impossible if Y_D had been the sole reductant in the fast phase. (Any reduced Y_D present after the flashes would have been consumed already by the S_3 state, and there would have been no reduced Y_D left to react with the S_2 state.) In addition, our experiments on the samples provided one flash clearly show that the "pure" S_2 state decays with two kinetics also in the absence of any reduced Y_D (Table 1). We conclude that the fast decay we describe here must have another origin than electron transfer from Y_D. The most straightforward explanation is that also the fast decay represents recombination with the acceptor side since electron transfer from known components on the donor side of PSII (Y_D and cytochrome b_{559}) can be discarded.

It is also interesting to compare the decay data for the S_2 state in samples given 1 or 2 flashes. In one case, the decay involves the S_2 state only while in the other case (after two flashes) the main part of S_2 is first formed via S_3 state decay. The kinetic behavior in both cases is strikingly similar (Table 1). The fast phase was found to be less temperature dependent while the slow phase was found to be dominating (about 90% in most cases) and temperature dependent. This is also holds for the S_3 state decay.What are then the processes behind these two decay phases which determine the stability of the S_3 and S_2 states? There are many possible reactions that in principle can participate in decay of these oxidized states in the Mn_4CaO_5 cluster. As analyzed in ref 51, the decay of the S states is likely to involve recombination between Q_A^- and P_{680}^+, both formed in redox equilibria on respectively the acceptor and donor side of PSII. The active recombination partner on the acceptor side is, most probably, Q_A^-. In our experiments, which are carried out in presence of an exogenous electron acceptor, Q_A^- is formed in equilibrium with reduced P*p*BQ. The similarities between the decay of the S_3 state and the decay of the S_2 state formed after one (directly) or two flashes (indirectly via S_3 state decay) indicate that this recombination partner (Q_A–P*p*BQ) behaves similarly in the recombination process in all S states and after different number of flashes (Scheme 1). On the donor side of PSII we can rule out involvement of reduced Y_D (see discussion above). Moreover, we have no indication of changes in the redox state of cytochrome b_{559}, which in principle could have acted as a slow donor to the higher S states (not shown). This leads to the hypothesis that reduction of respectively the S_3/Y_Z and S_2/Y_Z redox couples occurs via P_{680}^+ that is present in equilibrium with $Y_Z^\bullet$ as has been suggested in refs 47 and 48.

Scheme 1 shows two different models (1 and 2) that account for the biphasic decays of the S_3 and S_2 states (numerical fitting parameters are provided in the Supporting Information). To better discuss the models, it is necessary to first describe the forward electron transfer reactions involved on the donor side of PSII in some detail.[2] Following the primary charge separation, Y_Z reduces P_{680}^+ with S-state dependent kinetics. In the major fraction of centers (80–90% of PSII) the reduction occurs in the nanosecond time regime (Scheme 1, $t_{1/2}$AC). The nanosecond kinetics is essentially pH independent between pH 5.5 and 8.5, shows very small if any deuterium isotope effect, and is considered to be limited by electron transfer. This fast oxidation of Y_Z depends on a well-set hydrogen bond to His_Z which is shown in Scheme 2[52] and does not involve a large free energy drop.[1] In the remaining 10–20% of PSII oxidation of Y_Z occurs with 30–35 μs kinetics ($t_{1/2}$BD in model 1; $t_{1/2}$BA in model 2) that is pH dependent and shows a significant deuterium isotope effect indicating that the oxidation of Y_Z is limited by extensive movement of one or more protons. Both phases are considered to originate from functional PSII centers, and the very different kinetic behavior is considered to reflect the hydrogen bond system around Y_Z, including the hydrogen bond partner His_Z (Scheme 2, refs 2 and 52).

After formation, $Y_Z^\bullet$ is reduced from the Mn_4CaO_5 cluster leading to one-step advancement in the S cycle (Scheme 1,

dx.doi.org/10.1021/bi200627j | *Biochemistry* 2012, 51, 138–148

$t_{1/2}$CE). The kinetics are S-state dependent and slow down in the higher S states.[53] The reaction is driven far toward the formation of respective S state. Interestingly, there is experimental support for an equilibrium between the Mn_4CaO_5 cluster and Y_Z (eq 4). Here K_m is the equilibrium constant between Y_Z and respective S state and varies with S state and many experimental conditions. In most cases, the equilibrium is driven far toward reduction of $Y_Z^{\bullet}$. With electroluminescence measurements in thylakoid membranes, the presence of what seemed to be $Y_Z^{\bullet}$ was demonstrated in a small fraction of PSII centers when the S_3 and S_2 states had been already formed after the flash.[54] To explain this, it was suggested that Y_Z exists in equilibrium with the S_3 state (or in the some cases with the S_2 state) in this fraction of PSII (eq 4). After 1 or 2 flashes this results in the formation of a fraction of either $S_1Y_Z^{\bullet}$ or $S_2Y_Z^{\bullet}$ together with the dominating S_2 and S_3 states, respectively. Interestingly, this equilibrium shift exists independently on the situation on the acceptor side.[54] These measurements were carried out in osmotically swollen thylakoid membranes, at pH 7.8 and in the absence of an external electron acceptor. Although these conditions are very different from ours, this indicates that in the higher S-states (although the equilibrium is strongly displaced toward forward electron transfer) exist possibility for backward electron transfer between Y_Z and the Mn_4CaO_5 cluster allowing setup of the respective equilibrium:

$$S_iY_Z \overset{K_m}{\longleftrightarrow} S_{i-1}Y_Z^{\bullet} \quad (4)$$

Similar reactions, reflecting redox equilibria between Y_Z and the higher S states, have also been demonstrated by EPR spectroscopy. One interesting case is the observation that the S_3Y_Z state, by increasing the pH in the dark, is converted to a $S_2'Y_Z^{\bullet}$ state.[38,55] The pK_a for the conversion was reported to be about 8.5, and the reaction was shown to be reversible. It is clear that the pH used by de Wijn et al.[54] (pH 7.8) is in the pH range where this type of conversion should be observed. Reversible, backward electron transfer from Y_Z to the Mn_4CaO_5 cluster occurring via a redox equilibrium, again for both of the S_3 and S_2 states, has also been demonstrated at cryogenic temperatures.[26,56] This is the effect used in the present study where the split S_3 signal (presumably originating from $S_2'Y_Z^{\bullet}$) is induced by excitation of the Mn_4CaO_5 cluster with the NIR light.[26] Thus, it is clear that $Y_Z^{\bullet}$ exists with the S_3 state (or the S_2 state) in all, or at least a fraction, of the PSII centers. It is not clear what steers how large the concentration of $Y_Z^{\bullet}$ can be (K_m in eq 4), but from the data in ref 55 it is reasonable to suggest that the equilibrium is shifted toward Y_Z oxidation in a very large fraction of PSII at more elevated pH.

We suggest that factors which steer the equilibrium between Y_Z and the corresponding S state[57] determine the decay kinetics of the S_2 and S_3 states observed here. We assume that all decay reactions of the S_2 and S_3 states studied here reflect recombination between the acceptor side and P_{680}^+, which is present to some extent through equilibrium with $Y_Z^{\bullet}$.[47,48] Formation of $Y_Z^{\bullet}$ is determined by the equilibrium with the corresponding S state (eq 4, Scheme 1). The fast decay of the S_3 (and S_2) state occurs in 10−20% of the PSII centers while the remaining 80−90% decays in the slow reaction (Table 1). Thus, the fast decay of respective S state occurs in a similar fraction of centers as where electron transfer from Y_Z to P_{680}^+ occurs in the microsecond time domain while the slow decay occurs in a similar fraction of centers as where Y_Z works in the nanosecond time regime. It is tempting to correlate the two phenomena. In this case the difference between these two types of PSII centers could originate in the hydrogen bond situation around Y_Z. Scheme 1 shows two models that can account for this proposal while Scheme 2 shows how this could be connected to the hydrogen bond situation around Y_Z and His_Z.

In model 1 (Scheme 1) there are two functionally different populations of PSII (discussed in ref 58) present already before the arrival of the photon (intermediates G and H). Both populations are active in O_2 evolution. It is not impossible that these populations can be converted into each other, but they do not equilibrate with each other during the time scale of the experiment (k_{EF} and k_{FE} represent a very slow equilibrium on our experimental time scale, if at all existing). In 80−90% of PSII (denoted population I) reduction of P_{680}^+ by Y_Z occurs in the nanosecond time regime (k_{AC}) which is much faster than the recombination with the acceptor side (here denoted k_{AG}). In the other 10−20% of the centers (denoted II) the reduction of P_{680}^+ occurs with a 35 μs half-time (k_{BD}) which is only somewhat faster than the recombination reaction that probably also occurs in the micro second time regime (k_{BH}). The stepwise electron transfer equilibrium reactions in both branches are far displaced toward the $S_{(i+1)}$ state (bottom intermediates E and F). In pathway I, the recombination substrate P_{680}^+ (intermediate A) is depopulated very fast by reaction with Y_Z under any circumstance this is formed. Consequently, decay of the S_2 and S_3 states, which occurs via P_{680}^+, will be slow. The opposite holds for pathway II. Here, recombination of any formed P_{680}^+ will occur with a larger probability since the reduction from Y_Z (k_{BD}) is more comparable in rate to the recombination reaction (k_{BH}; note that there is no reason to suggest different recombination rates k_{AG} and k_{BH} between the two paths since the participating components are the same in pathways I and II). Consequently, in 80−90% of PSII the decay of the S_2 or S_3 state will be much slower than in the remaining 10−20% of PSII. This is what we have observed. On the right side in Scheme 1, we show a second model which can also account for the known observables (model 2). Here we have adopted to the hypothesis that the 35 μs kinetics in P_{680}^+ reduction represents 10−20% of PSII (population II) that is in equilibrium with the remaining PSII (population I) in a reaction where one of the reactions has a half-life of 35 μs.[2] The reactions in this equilibrium occur quite fast in presence of P_{680}^+. In model 2 we propose that a similar equilibrium exists in the presence of the $S_{(i+1)}$ state (intermediates E, F). However, to explain the very slow decay of the S_3 state (fast phase ca. 10 s and slow phase ca. 120 s; Table 1), this equilibrium must be very slow, occurring in the minute time scale (see Supporting Information for one numerical fit to the model). If this equilibrium is set in a much faster time scale, this results in monexponential decay of the S_3 state which would not be coherent with our data.

The fast and slow electron transfer from Y_Z to P_{680}^+ has been proposed to reflect the hydrogen bond situation around the phenolic proton on Y_Z which has to leave the tyrosine when this is oxidized.[2,31,52] It is thought that the fast nanosecond kinetics (Scheme 1, k_{AC}) and low-temperature oxidation of Y_Z occur when the proton is set in a well-tuned hydrogen bond to His_Z allowing very fast deprotonation while the slow microsecond kinetics reflect that hydrogen bond situation is less favorable. Scheme 2 shows these two situations and connects them to the two populations I and II in Scheme 1. This would suggest that the fast decay of the S_3 and S_2 states takes place in

PSII centers where the hydrogen bond between $Y_Z^{\bullet}$ and His_Z is not perfectly set. It is noteworthy that, if the fraction of centers participating in this equilibrium is pH dependent involving more centers at higher pH, this could also explain that Messinger et al. observed the fast decay phase of the S_3 and S_2 states in 28% and 35%, respectively, since their measurements were performed at pH 7.0.[46] The slow decay of the S_3 (and S_2) state then occurs in the remaining 80−90% of the PSII centers where the hydrogen bond between $Y_Z^{\bullet}$ and His_Z is well tuned to facilitate the forward electron transfer. Interestingly, the result is that the reverse reaction is not favored and the S_3 state decays by recombination that takes place in the several minutes time scale in our conditions.

We show here two models that account for the observation that the S_3 state decays with two kinetic components and connect these reactions with the populations of PSII where Y_Z oxidation occurs in nanoseconds or microseconds. One crucial difference is that model 1 assumes two populations of PSII that are not in equilibrium with each other in the time scale of the decay of the S_3 (and S_2) state while model 2 involves a very slow equilibrium between two populations of PSII when the OEC is in the S_3 (or S_2) state while it is fast immediately after the flash. We are presently designing experiments to test and select between these clearly differentiating aspects of the two models.

■ ASSOCIATED CONTENT

Supporting Information

Explanation and numerical simulations to the models described in the text and Scheme 1. This material is available free of charge via the Internet at http://pubs.acs.org.

■ AUTHOR INFORMATION

Corresponding Author

*Tel: +46 (0)18 471 6580; Fax: +46 (0)18 471 6844; e-mail: Stenbjorn.Styring@fotomol.uu.se.

Present Address

‡Department of Chemistry, Umeå University, Linnaeus väg 6, SE-901 87 Umeå, Sweden.

Author Contributions

†These authors contributed equally to the work.

Funding

This work was supported by the Swedish Research Council, the Swedish Energy Agency, the EU program SOLAR-H2 (FP7 contract no. 212508), and the Knut and Alice Wallenberg Foundation.

■ ABBREVIATIONS

Car, carotenoid; Chl, chlorophyll; EPR, electron paramagnetic resonance; His_Z, histidine 190 of the D1 protein of PSII; NIR, near-infrared; OEC, oxygen evolving complex; P_{680}, primary electron donor Chls in PSII; P*p*BQ, phenyl-*p*-benzoquinone; OEC, oxygen evolving complex; PSII, photosystem II; Q_A and Q_B, primary and secondary quinone acceptors of PSII; S states, intermediates in the cyclic turnover of the OEC; Y_D and $Y_D^{\bullet}$, tyrosine 161 of the D2 protein and its radical; Y_Z and $Y_Z^{\bullet}$, tyrosine 161 of the D1 protein and its radical.

■ ADDITIONAL NOTES

[a]The "room temperature" for these experiments was probably several degrees lower than the 18 °C given in the original reference[39] due to abnormally low room temperature during the time for the experiment (Styring, S., personal information). This temperature artifact in the original experiment was first noted in ref 9.

[b]We assume here that no PSII centers are in the S_0 state after the two flashes. This is reasonable since the two short flashes induced only S_2 and S_3 centers while any double hits leading to S_0 state formation can be excluded.

■ REFERENCES

(1) Rappaport, F., and Diner, B. A. (2008) Primary photochemistry and energetics leading to the oxidation of the $(Mn)_4Ca$ cluster and to the evolution of molecular oxygen in photosystem II. *Coord. Chem. Rev. 252*, 259−272.

(2) Renger, G. (2008) Functional pattern of photosystem II, in *Primary Processes of Photosynthesis−Part 2* (Renger, G., Ed.) pp 237−290, RSC Publishing, Cambridge, UK.

(3) McEvoy, J. P., and Brudvig, G. W. (2006) Water-splitting chemistry of photosystem II. *Chem. Rev. 106*, 4455−4483.

(4) Messinger, J., and Renger, G. (2008) Photosynthetic water splitting, in *Primary Processes of Photosynthesis−Part 2* (Renger, G., Ed.) pp 291−349, RSC Publishing, Cambridge, UK.

(5) Dau, H., and Haumann, M. (2008) The manganese complex of photosystem II in its reaction cycle—Basic framework and possible realization at the atomic level. *Coord. Chem. Rev. 252*, 273−295.

(6) Kok, B., Forbush, B., and McGloin, M. (1970) Cooperation of charges in photosynthetic O_2 evolution-I. A linear four step mechanism. *Photochem. Photobiol. 11*, 457−475.

(7) Junge, W., Clausen, J., Penner-Hahn, J. E., Yocum, F. C., Dau, H., and Haumann, M. (2006) Photosynthetic oxygen production. *Science 312*, 1470−1472.

(8) Dau, H., and Haumann, M. (2007) Eight steps preceding O-O bond formation in oxygenic photosynthesis − A basic reaction cycle of the photosystem II manganese complex. *Biochim. Biophys. Acta 1767*, 472−483.

(9) Vass, I., and Styring, S. (1991) pH-dependent charge equilibria between tyrosine-D and the S states in photosystem II. Estimation of relative midpoint redox potentials. *Biochemistry 30*, 830−839.

(10) Ferreira, K. N., Iverson, T. M., Maghlaoui, K., Barber, J., and Iwata, S. (2004) Architecture of the photosynthetic oxygen-evolving center. *Science 303*, 1831−1838.

(11) Loll, B., Kern, J., Saenger, W., Zouni, A., and Biesiadka, J. (2005) Towards complete cofactor arrangement in the 3.0 Å resolution structure of photosystem II. *Nature 438*, 1040−1044.

(12) Umena, Y., Kawakami, K., Shen, J.-R., and Kamiya, N. (2011) Crystal structure of oxygen-evolving photosystem II at a resolution of 1.9Å. *Nature 473*, 55−60.

(13) Miller, A. F., and Brudvig, G. W. (1991) A guide to electron paramagnetic resonance spectroscopy of photosystem II membranes. *Biochim. Biophys. Acta 1056*, 1−18.

(14) Petrouleas, V., Koulougliotis, D., and Ioannidis, N. (2005) Trapping of metalloradical intermediates of the S-states at liquid helium temperatures. Overview of the phenomenology and mechanistic implications. *Biochemistry 44*, 6723−6728.

(15) Haddy, A. (2007) EPR spectroscopy of the manganese cluster of photosystem II. *Photosynth. Res. 92*, 357−368.

(16) Havelius, K. G. V., Sjoholm, J., Ho, F. M., Mamedov, F., and Styring, S. (2010) Metalloradical EPR signals from the Y_Z·S-state intermediates in photosystem II. *Appl. Magn. Reson. 37*, 151−176.

(17) Kulik, L. V., Epel, B., Lubitz, W., and Messinger, J. (2005) ^{55}Mn pulse ENDOR at 34 GHz of the S_0 and S_2 states of the oxygen-evolving complex in photosystem II. *J. Am. Chem. Soc. 127*, 2392−2393.

(18) Dau, H., Liebisch, P., and Haumann, M. (2005) The manganese complex of oxygenic photosynthesis: Conversion of five-coordinated Mn(III) to six-coordinated Mn(IV) in the S_2-S_3 transition is implied by XANES simulations. *Phys. Scr. T115*, 844−846.

(19) Iuzzolino, L., Dittmer, J., Dorner, W., Meyer-Klaucke, W., and Dau, H. (1998) X-ray absorption spectroscopy on layered

photosystem II membrane particles suggests manganese-centered oxidation of the oxygen-evolving complex for the S_0-S_1, S_1-S_2, and S_2-S_3 transitions of the water oxidation cycle. *Biochemistry 37*, 17112–17119.

(20) Roelofs, T. A., Liang, W., Latimer, M. J., Cinco, R. M., Rompel, A., Andrews, J. C., Sauer, K., Yachandra, V. K., and Klein, M. P. (1996) Oxidation states of the manganese cluster during the flash-induced S-state cycle of the photosynthetic oxygen-evolving complex. *Proc. Natl. Acad. Sci. U. S. A 93*, 3335–3340.

(21) Messinger, J., Robblee, J. H., Bergmann, U., Fernandez, C., Glatzel, P., Visser, H., Cinco, R. M., McFarlane, K. L., Bellacchio, E., Pizarro, S. A., Cramer, S. P., Sauer, K., Klein, M. P., and Yachandra, V. K. (2001) Absence of Mn-centered oxidation in the $S_2 \rightarrow S_3$ transition: Implications for the mechanism of photosynthetic water oxidation. *J. Am. Chem. Soc. 123*, 7804–7820.

(22) Ono, T.-a., Noguchi, T., Inoue, Y., Kusunoki, M., Matsushita, T., and Oyanagi, H. (1992) X-ray detection of the period-four cycling of the manganese cluster in photosynthetic water oxidizing enzyme. *Science 258*, 1335–1337.

(23) Ioannidis, N., and Petrouleas, V. (2000) Electron paramagnetic resonance signals from the S_3 state of the oxygen-evolving complex. A broadened radical signal induced by low-temperature near-infrared light illumination. *Biochemistry 39*, 5246–5254.

(24) Ioannidis, N., and Petrouleas, V. (2002) Decay products of the S_3 state of the oxygen-evolving complex of photosystem II at cryogenic temperatures. Pathways to the formation of the S = 7/2 S_2 state configuration. *Biochemistry 41*, 9580–9588.

(25) Havelius, K. G. V., Su, J.-H., Feyziyev, Y., Mamedov, F., and Styring, S. (2006) Spectral resolution of the split EPR signals induced by illumination at 5 K from the S_1, S_3, and S_0 states in photosystem II. *Biochemistry 45*, 9279–9290.

(26) Havelius, K. G. V., Su, J.-H., Han, G., Mamedov, F., Ho, F. M., and Styring, S. (2011) The formation of the split EPR signal from the S_3 state of Photosystem II does not involve primary charge separation. *Biochim. Biophys. Acta 1807*, 11–21.

(27) Messinger, J., Wacker, U., and Renger, G. (1991) Unusual low reactivity of the water oxidase in redox state S_3 toward exogenous reductants. Analysis of the NH_2OH- and NH_2NH_2-induced modifications of flash-induced oxygen evolution in isolated spinach thylakoids. *Biochemistry 30*, 7852–7862.

(28) Messinger, J., and Renger, G. (1994) Analyses of pH-induced modifications of the period four oscillation of flash-induced oxygen evolution reveal distinct structural changes of the photosystem II donor side at characteristic pH values. *Biochemistry 33*, 10896–10905.

(29) Han, G., Ho, F. M., Havelius, K. G. V., Morvaridi, S. F., Mamedov, F., and Styring, S. (2008) Direct quantification of the four individual S states in photosystem II using EPR spectroscopy. *Biochim. Biophys. Acta 1777*, 496–503.

(30) Han, G., Mamedov, F., and Styring, S., unpublished experiments.

(31) Sjöholm, J., Havelius, K. G. V., Mamedov, F., and Styring, S. (2010) Effects of pH on the S_3 state of the oxygen evolving complex in photosystem II probed by EPR split signal induction. *Biochemistry 49*, 9800–9808.

(32) Dismukes, G. C., and Siderer, Y. (1981) Intermediates of a polynuclear manganese center involved in photosynthetic oxidation of water. *Proc. Natl. Acad. Sci. U. S. A. 78*, 274–278.

(33) Berthold, D. A., Babcock, G. T., and Yocum, C. F. (1981) A highly resolved, oxygen-evolving photosystem II preparation from spinach thylakoid membranes: EPR and electron-transport properties. *FEBS Lett. 134*, 231–234.

(34) Völker, M., Ono, T., Inoue, Y., and Renger, G. (1985) Effect of trypsin on PS-II particles. Correlation between Hill-activity, Mn-abundance and peptide pattern. *Biochim. Biophys. Acta 806*, 25–34.

(35) Styring, S., and Rutherford, A. W. (1987) In the oxygen-evolving complex of photosystem II the S_0 state is oxidized to the S_1 state by D^+ (signal II_{slow}). *Biochemistry 26*, 2401–2405.

(36) Åhrling, K. A., Peterson, S., and Styring, S. (1997) An oscillating manganese electron paramagnetic resonance signal from the S_0 state of the oxygen evolving complex in photosystem II. *Biochemistry 36*, 13148–13152.

(37) Su, J.-H., Havelius, K. G. V., Ho, F. M., Han, G., Mamedov, F., and Styring, S. (2007) Formation spectra of the EPR split signals from the S_0, S_1, and S_3 states in photosystem II induced by monochromatic light at 5 K. *Biochemistry 46*, 10703–10712.

(38) Bernat, G., Morvaridi, F., Feyziyev, Y., and Styring, S. (2002) pH dependence of the four individual transitions in the catalytic S-cycle during photosynthetic oxygen evolution. *Biochemistry 41*, 5830–5843.

(39) Styring, S., and Rutherford, A. W. (1988) Deactivation kinetics and temperature dependence of the S-state transitions in the oxygen-evolving system of photosystem II measured by EPR spectroscopy. *Biochim. Biophys. Acta 933*, 378–387.

(40) Feyziyev, Y., Rotterdam, B. J. v., Bernát, G., and Styring, S. (2003) Electron transfer from cytochrome b_{559} and $tyrosine_D$ to the S_2 and S_3 states of the water oxidizing complex in photosystem II. *Chem. Phys. 294*, 415–431.

(41) Zimmermann, J. L., and Rutherford, A. W. (1986) Photoreductant-induced oxidation of Fe^{2+} in the electron-acceptor complex of photosystem II. *Biochim. Biophys. Acta 851*, 416–423.

(42) Joliot, P., Joliot, A., Bouges, B., and Barbieri, G. (1971) Studies of System-II photocenters by comparative measurements of luminescence fluorescence, and oxygen emission. *Photochem. Photobiol. 14*, 287–305.

(43) Bouges-Bocquet, B., Bennoun, P., and Taboury, J. (1973) Deactivation of oxygen precursors in presence of 3(3,4-dichlorophenyl)-1,1-dimethylurea and phenylurethane. *Biochim. Biophys. Acta 325*, 247–254.

(44) Renger, G., Bouges-Bocquet, B., and Delosme, R. (1973) Studies on the ADRY agent-induced mechanism of the discharge of the holes trapped in the photosynthetic waterspliting enzyme system Y. *Biochim. Biophys. Acta 292*, 796–807.

(45) Vermaas, W. F. J., Renger, G., and Dohnt, G. (1984) The reduction of the oxygen-evolving system in chloroplasts by thylakoid components. *Biochim. Biophys. Acta 764*, 194–202.

(46) Messinger, J., Schroeder, W. P., and Renger, G. (1993) Structure-function relations in photosystem II. Effects of temperature and chaotropic agents on the period four oscillation of flash-induced oxygen evolution. *Biochemistry 32*, 7658–7668.

(47) Buser, C. A., Diner, B. A., and Brudvig, G. W. (1992) Photooxidation of cytochrome b_{559} in oxygen-evolving photosystem II. *Biochemistry 31*, 11449–11459.

(48) Buser, C. A., Thompson, L. K., Diner, B. A., and Brudvig, G. W. (1990) Electron-transfer reactions in manganese-depleted photosystem II. *Biochemistry 29*, 8977–8985.

(49) Isgandarova, S., Renger, G., and Messinger, J. (2003) Functional differences of photosystem II from *Synechococcus elongatus* and spinach characterized by flash induced oxygen evolution patterns. *Biochemistry 42*, 8929–8938.

(50) Deak, Z., Vass, I., and Styring, S. (1994) Redox interaction of tyrosine-D with the S-states of the water-oxidizing complex in intact and chloride-depleted photosystem II. *Biochim. Biophys. Acta 1185*, 65–74.

(51) Rappaport, F., Guergova-Kuras, M., Nixon, P. J., Diner, B. A., and Lavergne, J. (2002) Kinetics and pathways of charge recombination in photosystem II. *Biochemistry 41*, 8518–8527.

(52) Styring, S., Sjöholm, J., and Mamedov, F. (2011) Two tyrosines that changed the world: Interphasing the oxidizing power of photochemistry to water splitting in photosystem II. *Biochim. Biophys. Acta*, DOI: 10.1016/j.bbabio.2011.03.016.

(53) Reza Razeghifard, M., and Pace, R. J. (1997) Electron paramagnetic resonance kinetic studies of the S states in spinach PSII membranes. *Biochim. Biophys. Acta 1322*, 141–150.

(54) de Wijn, R., Schrama, T., and van Gorkom, H. J. (2001) Secondary stabilization reactions and proton-coupled electron transport in Photosystem II investigated by electroluminescence and fluorescence spectroscopy. *Biochemistry 40*, 5821–5834.

(55) Geijer, P., Morvaridi, F., and Styring, S. (2001) The S_3 state of the oxygen-evolving complex in photosystem II is converted to the $S_2Y_Z^{\bullet}$ state at alkaline pH. *Biochemistry 40*, 10881−10891.
(56) Koulougliotis, D., Shen, J.-R., Ioannidis, N., and Petrouleas, V. (2003) Near-IR irradiation of the S_2 state of the water oxidizing complex of photosystem II at liquid helium temperatures produces the metalloradical intermediate attributed to $S_1Y_Z^{\bullet}$. *Biochemistry 42*, 3045−3053.
(57) Gasanov, R., Aliyeva, S., Arao, S., Ismailova, A., Katsuta, N., Kitade, H., Yamada, S., Kawamori, A., and Mamedov, F. (2007) Comparative study of the water oxidizing reactions and the millisecond delayed chlorophyll fluorescence in photosystem II at different pH. *J. Photochem. Photobiol., B 86*, 160−164.
(58) Kühn, P., Eckert, H.-J., Eichler, H. J., and Renger, G. (2004) Analysis of the $P680^+$ reduction pattern and its temperature dependence in oxygen-evolving PS II core complexes from thermophilic cyanobacteria and higher plants. *Phys. Chem. Chem. Phys. 6*, 4838−4843.